# A Quinoline-Based DNA Methyltransferase Inhibitor as a Possible Adjuvant in Osteosarcoma Therapy

**Maria Cristina Manara[1*], Sergio Valente[2*], Camilla Cristalli[1], Giordano Nicoletti[1], Lorena Landuzzi[1], Clemens Zwergel[2], Roberta Mazzone[2,3], Giulia Stazi[2], Paola B. Arimondo[4**], Michela Pasello[1], Clara Guerzoni[1], Piero Picci[1], Patrizia Nanni[5], Pier-Luigi Lollini[5], Antonello Mai[2,6], Katia Scotlandi[1].**

[1]Laboratory of Experimental Oncology, Orthopaedic Rizzoli Institute, Via Di Barbiano 1/10, 40136 Bologna, Italy; [2]Department of Chemistry and Technologies of Drugs, "Sapienza" University of Rome, P. le A. Moro 5, 00185 Rome, Italy; [3]Center for Life NanoScience@Sapienza, Italian Institute of Technology, Viale Regina Elena 291, 00161 Rome, Italy; [4]ETaC, Epigenetic Targeting of Cancer, CRDPF, CNRS-Pierre Fabre USR3388, 3 Avenue H. Curien, 31035 Toulouse cedex 01, France; [5]DIMES, Department of Experimental, Diagnostic and Specialty Medicine, University of Bologna, Bologna, Italy; [6]Istituto Pasteur-Fondazione Cenci Bolognetti, University "La Sapienza", P. le A. Moro 5, 00185 Rome, Italy

**Running title**: Effects of the DNMT inhibitor MC3343 in osteosarcoma

**Keywords:** epigenetics; DNMT inhibitor; osteosarcoma; anticancer agent

**Corresponding author:** Katia Scotlandi, CRS Development of Biomolecular Therapies, Experimental Oncology Laboratory, Rizzoli Orthopaedic Institute, via di Barbiano 1/10, 40136 Bologna, Italy. E-mail: katia.scotlandi@ior.it

**Co-corresponding author:** Antonello Mai, Sapienza University of Rome, P.le A. Moro 5, 00185 Roma, Italy. E-mail: antonello.mai@uniroma1.it

* The authors equally contributed to the work

** current affiliation:
Epigenetic Chemical Biology
Institut Pasteur Bât Lwoff 28 rue du docteur Roux 75274 Paris cedex 14

## Acknowledgments

This work was funded by AIRC (IG 18451 to K. Scotlandi; IG 19162 to A. Mai), the Italian Ministry of Health (TRANSCAN_ project TORPEDO_ER-2015-23604059 to K. Scotlandi), Progetto Ateneo Sapienza (to A. Mai), PRIN 2016 (prot 20152TE5PK to A. Mai), and the NIH (R01GM114306 to A. Mai).

The authors thank Cristina Ghinelli for editing the manuscript

**Disclosure of potential conflicts of interest:** The authors declare no conflict of interest.

## Abstract

The identification of new therapeutic strategies against osteosarcoma (OS), the most common primary bone tumor, continues to be a primary goal to improve the outcomes of patients refractory to conventional chemotherapy. OS originates from the transformation of mesenchymal stem cells (MSCs) and/or osteoblast progenitors, and the loss of differentiation is a common biological OS feature which strong significance in predicting tumor aggressiveness. Thus, restoring differentiation through epigenetic reprogramming is potentially exploitable for therapeutic benefits. Here, we demonstrated that the novel non-nucleoside DNMT inhibitor (DNMTi) MC3343 affected tumor proliferation by blocking OS cells in G1 or G2/M phases and induced osteoblastic differentiation through the specific re-expression of genes regulating this physiological process. While MC3343 has a similar antiproliferative effect as 5azadC, the conventional FDA-approved nucleoside inhibitor of DNA methylation, its effects on cell differentiation are distinct. Induction of the mature osteoblast phenotype coupled with a sustained cytostatic response was also confirmed *in vivo* when MC3343 was used against a patient-derived xenograft (PDX). In addition, MC3343 displayed synergistic effects with doxorubicin (DXR) and cisplatin (CDDP), two major chemotherapeutic agents used to treat OS. Specifically, MC3343 increased stable DXR bonds to DNA, and combined treatment resulted in sustained DNA damage and increased cell death. Overall, this non-nucleoside DNMTi is an effective novel agent and is thus a potential therapeutic option for OS patients who respond poorly to pre-adjuvant chemotherapy.

## Introduction

Osteosarcoma (OS), the most common primary bone tumor, occurs mainly in children and adolescents and therefore has an important social impact despite its rarity (1). To date, the most effective therapeutic strategy against OS is surgical resection combined with chemotherapy (2, 3). This multidisciplinary approach has increased the survival of patients with localized tumors over the past few decades, achieving a 5-year survival rate of up to 70% (4, 5). However, outcomes for patients with metastasis at diagnosis or for those who fail first-line treatment remain unsatisfactory (6). The multiple and complex genetic aberrations that characterize OS have prevented the identification of specific, common oncogenic drivers (7) and the successful application of targeted therapies, thwarting any improvement in survival (8). The adoption of immunotherapy with checkpoint inhibitors may also be relevant in the treatment of patients with sarcomas, as an increasing number of successes in other tumors have been reported. Such impressive results, however, have not been replicated in OS, and novel therapeutic approaches are therefore urgently needed. OS is thought to originate from the transformation of mesenchymal stem cells (MSCs) and/or osteoblast progenitors in any phase of differentiation (9). Transformation generates a block in normal development coupled with abnormal proliferation processes, and differentiation loss is a widespread biological feature of these tumors and has a strong prognostic significance (10). Thus, restoring differentiation by unlocking the stops driven by genetic and epigenetic alterations may be exploited as a therapeutic opportunity. Several lines of evidence have indicated that chromatin modifications in cancer versus normal MSCs include increased gene-specific DNA methylation and increased histone methylation, while the loss of DNA methylation occurs in normal processes of MSC differentiation [for a review see (11)]. Here, we analyzed the effects of a novel non-nucleoside DNA methyltransferase inhibitor (DNMTi), the N-(3-(2-amino-6-methylpyrimidin-4-ylamino)phenyl)-3-(quinolin-4-ylamino)benzamide MC3343, on cell proliferation, survival and differentiation in a representative panel of OS patient-derived cell lines and xenografts. DNA hypermethylation is a common feature in tumor development. In humans, DNA methylation occurs at the C-5 position of cytosines, mainly in a CpG dinucleotide context, and is catalyzed by members of the DNMT family of enzymes that transfer a methyl group from S-adenosyl-methionine (AdoMet) to the DNA cytosine C5 (12, 13). Catalytically active DNMTs (DNMT1, DNMT3a and DNMT3b) share common features, especially a regulatory N-terminal

domain and a catalytic C-terminal domain, which are conserved among different species. DNMT1, the first purified and characterized and most abundant DNMT in somatic cells, has a greater affinity for hemi-methylated DNA rather than un-methylated DNA. DNMT1 acts mainly after DNA replication to methylate the newly synthesized strand and is typically known as a maintenance methyltransferase (13). DNMT1 is essential during developmental stages and in adult somatic cells to ensure cell proliferation and survival (14). In cancer cells, disruption of DNMT1, either genetically or pharmacologically through the use of DNMTis, is sufficient to stop the growth of tumors (12), reverse the un-differentiated state, and inhibit the invasiveness of cells, thus providing a very interesting therapeutic target (15). DNMTis are currently classified as nucleoside analogs, such as azacitidine (5azaC, Vidaza®) and decitabine (5azadC,Dacogen®), or non-nucleoside obtained by repositioning old drugs (e.g., hydralazine, procainamide, curcumin, and epigallocatechin gallate) or by identifying new drugs (e.g., RG-108, nitrophenyl-flavones, Δ2-isoxazolines, and SGI-1027) (12, 16). The first category of drugs has been approved for the treatment of myelodysplasia and several solid tumors including some cases of neuroblastoma, despite their poor bioavailability, chemical instability and toxic side effects (17-19). To date, DNMTis have been scarcely investigated in OS; most existing studies involve two approved nucleoside inhibitors, 5azaC and 5azadC (4, 20-25), and scarce data are available regarding non-nucleoside DNMTis. To improve the efficacy and DNMT-selectivity of non-nucleoside analogs, we chemically manipulated the SGI-1027 structure (26) by preparing all of its regioisomers, as well as some truncated and symmetric bis-quinoline and bis-pyrimidine analogs to test against DNMT1 and DNMT3a, and identified MC3343 as the best inhibitor (27). MC3343 is a strong DNA binder, showing preferential binding to DNA in CG-rich regions, and destabilizes the DNMT1-AdoMet DNA complex (28). Here, MC3343 efficiently inhibited OS cell proliferation, induced the specific re-expression of osteoblastogenesis genes, and acted synergistically with doxorubicin (DXR) and cisplatin (CDDP). We found that MC3343 improved the accessibility of DXR to DNA and significantly increased DXR-induced DNA damage and cell death.

## Materials and Methods

### Chemicals

MC3343 was prepared as previously reported (27, 28). 5azadC was purchased from Sigma-Aldrich . Stock solutions were prepared in DMSO and stored at −20°C.

### DNMT1 and DNMT3a assays in a cell-free context

DNMT1 and DNMT3a enzyme inhibition assays were performed according to Valente et al. (27). A detailed description is provided in the Supplementary Materials and Methods.

### DNMT activity assay in a cell context

DNMT activity was measured using an EpiQuik DNA Methyltransferase Activity/Inhibition Kit (Epigentek). Cells were treated with MC3343 (1-10 μM) or 5azadC (0.1-10 μM) for 48 h, and 5 μg of nuclear extracts isolated using the EpiQuik Nuclear Extraction Kit (Epigentek) was added to each reaction well according to the manufacturer's protocol. Absorbance was determined using a microplate spectrophotometer at 450 nm (GloMax luminometer, Promega). The data are expressed as the mean ± SE of three independent experiments.

### Cell lines

The patient-derived human OS cell lines Saos-2, U-2OS and MG-63 were obtained from American Type Culture Collection (1992). The patient-derived OS cell lines IOR/OS9, IOR/OS10, IOR/OS14, IOR/OS20, and IOR/SARG were established and previously characterized at the Laboratory of Experimental Oncology of Rizzoli Orthopedic Institute (29). Cell lines were profiled for the DNA copy number changes (30) and DNA methylation status at approximately 27,000 CpG sites (31). The cell lines PDX-OS#1-C4 and PDX-OS#2-C2 were obtained from OS patient-derived xenografts (PDXs) after four or two passages in the animal, respectively (2015). All cell lines were tested for mycoplasma contamination (Mycoalert Mycoplasma Detection Kit, Lonza) before use and authenticated by short-tandem repeat polymerase chain reaction (STR PCR) analysis; detailed information is provided in the Supplementary Materials and Methods. All cell lines were immediately amplified to constitute liquid nitrogen stocks and were never passaged for more than 1 month upon thawing. Cells were maintained in Iscove's Modified Dulbecco's Medium (IMDM) supplemented with 10% heat-inactivated FBS (Lonza), penicillin (20 U/mL) and streptomycin (100 μg/mL) (Sigma-Aldrich) in a 37°C humidified at 5% $CO_2$.

**Cell culture experiments**

To perform cell culture experiments, $2x10^5$ cells/well were plated, and DNMTi MC3343 (1-30 µM) or 5azadC (0.1-30 µM) was added after 24 h. Cells were exposed for up to 96 h before being counted by Trypan blue vital cell count (Sigma-Aldrich). In parallel, cells were treated with DMSO-containing medium as a control. The highest final concentration of DMSO in the medium was $\leq$0.005%, and DMSO had no effect on cell growth inhibition. In combination experiments, cells were treated for 96 h with MC3343 alone (control) or in combination with a fixed ratio of DXR (Pfizer), CDDP (Sandoz) and methotrexate (MTX, Sigma-Aldrich). For cell cycle analysis after 24-48 h of treatment, 5-bromo-2'-deoxyuridine (BrdU, Sigma-Aldrich) labeling was used to assess cell proliferation. Then, the cells were processed for indirect immunofluorescence staining using anti-BrdUmAb (1:8; BD-Biosciences, #347580) as a primary antibody, anti-mouse FITC as a secondary antibody (1:100; Thermo Scientific, #31569) and 20 µg/mL propidium iodide for the analysis of DNA content before flow cytometry analysis (Sysmex, Partec). To measure the intranuclear uptake of DXR, living cells were exposed to DXR (1-10 µM for 30-60 min at 37°C) (32) with or without MC3343 (10 µM) or 5azadC (1 µM). γ-H2AX expression and quantification was assessed by flow cytometry after staining with an anti-γH2AX antibody (Ser139, 1:50, Cell Signaling Technology, #9718) and anti-rabbit FITC as a secondary antibody (1:80; DAKO, #F0205).

Short interfering RNA (siRNA)-mediated knockdown of DNMT1 and DNMT3a was performed with siRNAs from Thermo Scientific Dharmacon; SMART POOL siGENOME_siRNA (FE5M004605010020 for DNMT1 and FE5M006672030020 for DNMT3a). siGENOME_non targeting_siRNA was used as control (FE5D0012061320). siRNAs (25 nM and 50 nM) were transfected into Saos-2 and PDX-OS#1-C4 cells using the transfection agent TransIT-x2 System (Mirus, #MIR6000) according to the manufacturer's instructions. For details please refer to Supplementary Material and Methods.

**OS differentiation toward osteoblasts**

Four days after seeding, OS cells were exposed to specific osteogenic medium (IMDM supplemented with 2% FBS, 5 mM β-glycerophosphate and 50 µg/mL ascorbic acid, Sigma-Aldrich) without (control) or with MC3343 (1-5 µM) or 5azadC (0.1-0.5 µM) and maintained in differentiating conditions for up to 21 days. The medium was renewed every 4 days, and cells were harvested at various time points to collect total RNA and verify bone mineralization. Specific osteoblastic markers were evaluated by quantitative real-time PCR (RT-qPCR) as previously

described (33). The primers or assays (Applied Biosystems) used are as follows: GAPDH forward: 5'-GAAGGTGAAGGTCGGAGTC-3', reverse: 5'-GAAGATGGTGATGGGATTTC-3' and probe: 5'-CAAGCTTCCCGTTCTCAGCC-3'; OCN, forward: 5'-GGGCTCCCAGCCATTGAT-3' and reverse: 5'-CAAAGCCTTTGTGTCCAAGCA-3'; ALPL (Hs01029144_m1); and COL1A2 (Hs01028970_m1). Amplification reactions were performed using a ViiA7™ Real-Time PCR System (Life Technologies). Osteoblastic differentiation was assessed after 7-14 days by alkaline phosphatase (ALPL) staining using a Leukocyte Alkaline Phosphatase Kit (Sigma-Aldrich) according to the manufacturer's instructions. To visualize bone mineralization, the plates were stained with 40 mM Alizarin red stain (ARS, Sigma-Aldrich). ARS was extracted from the monolayer and transferred to a 96-well plate for reading at 550 nm (GloMax luminometer, Promega). For a more general view of the osteogenic differentiation of OS cells, the Human Osteogenesis RT2 Profiler PCR Array (Qiagen-SA Biosciences) was used.

**Immunofluorescence staining**

Cells were seeded on coverslips and treated with increasing concentrations of MC3343 for up to 72 h, fixed with 4% paraformaldehyde and permeabilized with 0.15% Triton X-100/PBS. The samples were incubated with anti-DNMT1 (sc-271729), anti-DNMT3a (sc-20703), anti-DNMT3b (sc-130740) antibodies (1:50, Santa Cruz) or with an MIB-1 antibody (1:50; Calbiochem-Novabiochem, NA21-2) and visualized with an ECLIPSE 90i microscope (Nikon, Tokyo, Japan) equipped with Plan Apo VC 60X oil NA 1.4. Images were captured under identical conditions using a digital color camera (Nikon DS5 MC) and NIS-Elements AR3.10 software (Nikon). The percentage of Ki-67-positive cells in samples of at least 500 cells was quantified and expressed as the Ki-67 labeling index (LI).

**Western blotting**

Subconfluent cells were treated as described above and processed for Western blotting following standard procedures. The following primary antibodies were used: anti-DNMT1 (1:1000, Bethyl Laboratories, A300-041A-M); anti-DNMT3a (1:1000, sc-20703), anti-DNMT3b (1:1000, sc-130740), anti-Cyclin D1 (1:2000, sc-753), and anti-GAPDH (1:5000, sc-25778) (all purchased from Santa Cruz Biotechnology); anti-pRbs (S807/811, S795, 1:1000, Rb sampler kit, #9969); anti-Rb (1:1000, #9309); anti-PARP (1:1000, #9542); and anti-cleaved caspase-3 (Asp175, 1:500, #9661) (all from Cell Signaling Technology); and anti-actin (1:1000, Merck Millipore, MAB1501). Anti-rabbit or anti-

mouse secondary antibodies conjugated to horseradish peroxidase (1:1000-1:20000, GE Healthcare) were used, and bands were visualized with enhanced chemiluminescence (ECL) western blotting detection reagents (EuroClone).

**Patient-derived xenografts (PDXs) from primary human OS and *in vivo* treatments**

Rag 2-/-; Il2rg-/- breeders were kindly provided by Drs. T. Nomura and M. Ito of the Central Institute for Experimental Animals (Kawasaki, Japan) (34). Mice were then bred in our animal facilities under sterile conditions. Male mice aged 5-11 weeks, were used to generate PDXs by subcutaneous xenografts of OS fragments at the level of interscapular brown fat. PDX-OS#1 was derived from a primary high-grade osteoblastic OS. Pharmacological treatments began when the tumor reached a volume of 0.01 $cm^3$. Tumor size was measured using a caliper, and tumor volume was calculated according to the following formula: tumor volume=$\pi[\sqrt{}(a\times b)]^3/6$, where a =maximal tumor diameter and b=tumor diameter perpendicular to a. The animals were randomized to receive intraperitoneal injections of 0.8 mg/kg 5azadC, peritumoral injections of 20 mg/kg MC3343 or the vehicle control (PBS:DMSO 1:1) 5 days a week. DXR was administered intraperitoneally for two consecutive days (50 µg/injection). Mouse body weights and tumor volumes were measured at least once a week.

**Immunohistochemistry and von Kossa staining**

An avidin-biotin-peroxidase procedure was used to immunostain formalin-fixed, paraffin-embedded PDX cells. After antigen retrieval with a citrate buffer solution (pH 6.0), the slides were stained with an MIB-1 antibody (1:100; Calbiochem-Novabiochem, NA21-2) or anti-DNMT1 (1:50; Santa Cruz, sc-271729).

To visualize calcium deposits, von Kossa staining was performed. Tissue sections were treated with a 2% silver nitrate solution (Sigma-Aldrich) according to the manufacturer's protocol and counterstained with Nuclear Fast Red (Sigma-Aldrich).

**Statistical analyses**

The data are presented as the mean ± SE for *in vitro* and *in vivo* studies. Correlations between two variables were obtained by Pearson's test, and $IC_{50}$ (concentration required to inhibit cell proliferation by 50%) values were calculated from the linear transformation of dose-response curves. To define drug–drug interactions (synergism: combination index (CI) < 0.9; additivity: 0.90

< CI < 1.10; antagonism: CI > 1.10) (35) CalcuSyn software (Biososoft) was used. Differences among means were analyzed by Student's t tests or chi square tests.

**Ethics statement**

Animal experiments were performed following the European directive 2010/63/UE and Italian law DL 26/2014. Experimental protocols were reviewed and approved by the Institutional Animal Care and Use Committee ("Comitato per il Benessere Animale") of the University of Bologna and the Italian Ministry of Health with letter 782/2015-PR (Responsible Researcher Prof. Patrizia Nanni). The ethics committee of the Rizzoli Institute approved the studies (0018587/2016) and patient-informed consent forms were obtained for the establishment of PDX models,.

## Results

### The non-nucleoside DNMTi MC3343 efficiently inhibits OS cell proliferation and induces osteoblastic differentiation

In cell-free assays, MC3343 displayed increased potency against DNMT1 compared with RG-108 and SGI-1027, with an $EC_{50}$ (effective concentration needed to inhibit 50% of the enzyme effect) of 5.7 µM, which is 68-fold more potent than RG-108 and 2-fold more effective than SGI-1027. Against DNMT3a, the potency ($EC_{50}$ = 1.7 µM) of MC3343 was 290-fold higher than that of RG-108 but 2-fold less than that of SGI-1027 (Supplementary Table S1) (27). In the representative Saos-2 OS cells, MC3343 induced dose- and time-dependent decreases in DNMT1, DNMT3a and DNMT3b protein levels (Fig. 1A-B) as well as enzyme activity (Fig. 1C). The effects were similar to those observed after treatments with the well-known nucleoside analog demethylating agent 5azadC (Fig. 1). Ten human OS cell lines, 8 derived directly from patients and 2 from PDX-OS mouse models, were exposed to MC3343, and the results were compared with those of 5azadC (Table 1). The $IC_{50}$ values ranged from 5-15 µM for MC3343 and from 0.5- to->30 µM for 5azadC. Sensitivity to MC3343 inversely correlated with the expression of DNMT1 and DNMT3a (r=-0.640 or -0.637, respectively, $p<0.05$, Pearson's correlation test), and this inverse relationship was not observed for 5azadC. To sustain the specific effects of DNMT inhibition on OS cell growth, we also silenced DNMT1, DNMT3a, or both and verified the impact on Saos-2 growth under standard conditions (Supplementary Fig. S1A- B).

Analysis of the cell cycle and apoptosis indicated that both MC3343 and 5azadC slowed cell proliferation (Ki-67) (Fig. 2A) and, accordingly, induced cyclin D1 downregulation and decreased the phosphorylation of the retinoblastoma gene product (pRb) (Fig. 2B). Cell cycle analysis indicated that MC3343 increased the percentage of cells in G0/G1 or G2/M phases of the cell cycle

(Fig. 2C), confirming its antiproliferative effect. In contrast, no induction of apoptosis was observed for either MC3343 or 5azadC. Along with the loss of expression of many genes encoding cell cycle regulators, epigenetic modifications also have pronounced effects on regulating cell fate and differentiation. To investigate the effects of MC3343 on OS differentiation, we took advantage of the osteoblastic-like Saos-2 OS cell line, which can differentiate toward an osteogenic lineage when maintained in low-serum medium supplemented with ascorbic acid (50 µg/mL) and β-glycerophosphate (5 mM) (36). Osteoblasts produce and secrete proteins that constitute bone matrix, such as collagens and osteocalcin (OCN), and are essential for osteoid extracellular matrix (ECM) mineralization, a process mediated by alkaline phosphatase (ALPL). Accordingly, we evaluated the effects of MC3343 on the expression of osteoblast differentiation genes, such as collagen type I alpha 2 chain (COL1A2), ALPL and OCN, by RT-qPCR; these data were analyzed together with the amount of mineralized ECM evaluated by ARS staining. In total, 1 µM of MC3343 (corresponding to the IC30 values) inhibited cell proliferation and significantly increased ECM mineralization (Fig. 3A and B). Moreover, we demonstrated decreased expression of COL1A2, an early marker of osteoblast differentiation, and upregulation of ALPL and OCN, markers of intermediate and terminal differentiation, respectively (Fig. 3C and D). Notably, 5azadC had a similar effect on cell proliferation but was unable to drive OS cells towards a specific differentiation profile. After exposure to 5azadC, Saos-2 cells did not mineralize *in vitro* (Fig. 3B), and ALPL and other osteoblastic markers were unmodified (Fig. 3C and D). To further confirm that the effects of MC3343 are indeed due to specific inhibition of DNMT, we silenced DNMTs using siRNAs and verified that DNMT deprivation under differentiating conditions inhibited cell proliferation (Supplementary Fig. S1C) and induced osteoblastic differentiation, as shown by increased ALPL activity and matrix mineralization (Supplementary Fig S1D and E). The different effects of MC3343 and 5azadC on differentiation were confirmed in a cell line derived from a PDX-

OS (PDX-OS#1-C4) (Fig. 3C and D) and were even clearer with the Human Osteogenesis RT² Profiler™ PCR Array, which allows for a quick and reliable gene expression analysis of 84 genes related to osteogenic differentiation. Under differentiating conditions on day 7, exposing Saos-2 cells to MC3343 induced the expression (>1.4-fold) of several genes involved in ossification. In particular, activation of several osteoblastic differentiating mediators was evident, including augmented bone morphogenetic proteins (BMPs; increased BMP1, BMP2, and BMP 5) and receptors (BMPR1A, 1B); upregulated growth factors involved in the early induction of osteoblastogenesis, such as basic fibroblast growth factor 2 (FGF2), receptor activator of nuclear factor kappa-B ligand (TNFSF11) and insulin-like growth factor 1 (IGF1); increased transcriptional factors (SOX9, TWIST1 and SPP1); and bone gamma-carboxyglutamate protein (BGLAP, also known as OCN), which encodes a highly abundant bone protein secreted by osteoblasts that regulates bone remodeling (Supplementary Table S2). In addition, MC3343 repressed chordin (CHRD), which encodes a secreted BMP antagonist protein, resulting in enhanced bone regeneration. Gene repression was also observed for matrix metallopeptidase 10 (MMP10), growth differentiation factor 10 (GDF10) and vascular endothelial growth factor receptor (FLT1), which are all involved in tumor malignancy. Globally, 30 genes were found to be upregulated and 8 genes were repressed after MC3343 exposure (Supplementary Table S2). In contrast, 5azadC induced generalized but rather undefined re-expression of the genes (76/84, 90% induced; 0/84, 0% repressed). Differences between the two agents were more evident on day 14, where MC3343 repressed 19/84 genes and induced only 8/84 genes, while 5azadC continued to induce generalized re-expression of the genes (65/84, 77%). Specifically, repression induced by MC3343 involved genes expressed in chondrocytes or osteoclasts, such as those encoding cartilage oligomeric matrix protein (COMP), type I collagens, and calcitonin receptor (CALCR), indicating that the compound

specifically drives OS cells toward the osteoblast fate. In contrast, all these genes were upregulated by 5azadC, supporting its undefined action (Supplementary Table S2).

**MC3343 reduces PDX OS growth and induces differentiation**

Given that PDXs preserve the tumor genomic profiles of patients and cancer biology better than patient-derived cell lines (37), the therapeutic potential of MC3343 was investigated against PDX-OS#1 xenografts. Mice were treated with 20 mg/kg MC3343 or 0.8 mg/kg 5azadC when a tumor volume of 0.01 $cm^3$ was reached. Peritumoral MC3343 administration was chosen as the first attempt to achieve a higher local concentration and test the direct activity of only the drug and not its metabolites. MC3343 was well tolerated, with no significant changes in mouse weights (Supplementary Fig. S2A), and significantly reduced tumor growth, which reproduced the effects observed with 5azadC (Fig. 4A, $p<0.05$ Student's t test). The significant inhibition of cell proliferation was confirmed by Ki-67 evaluation (Fig. 4B). Consistent with the *in vitro* data, only MC3343, not 5azadC was able to drive osteoblast differentiation, despite their similar effects on cell growth. Osteoblast differentiation was proven by von Kossa staining for calcium deposits and increased OCN positivity after MC3343 treatment (Fig. 4C). Mineralized matrix induction by MC3343 may have limited the shrinkage of the tumors, which resulted in their having dimensions similar to those treated with 5azadC, masking the additional value of the compound.

**MC3343 synergizes with DXR and CDDP in OS cells**

*In vitro*, MC3343 was found to synergize with DXR and CDDP (CI: 0.580±0.02 for DXR; CI= 0.784±0.01 for CDDP) but not MTX (CI: 1.317±0.08) in PDX-OS#1-C4, 5azadC induced sub-additive effects when combined with DXR (CI: 1.500±0.254), while silencing of DNMT1 or DNMT3a potentiated the cytotoxic effects of DXR ($IC_{50}$ values: 18.05±4.27 ng/ml when cells were

transfected with SCR vs 2.40±0.42 ng/ml or 1.79±0.58 ng/ml when cells were silenced for DNMT1 or DNMT3a, respectively) again mirroring the effects of MC3343 (Supplementary Fig. S1G) The advantage of using combined treatments was confirmed *in vivo*, when MC3343 was administered in combination with DXR (Fig. 5A). Tumor growth was significantly inhibited when both drugs were administered together, with improved efficacy being observed compared to the single agents. Reduced body weights were observed in mice receiving the combined treatment (Supplementary Fig. S2B).

As recently observed (38, 39), epigenetic drugs are capable of increasing chromatin accessibility to conventional chemotherapeutic agents, significantly enhancing their effects. Taking advantage of DXR autofluorescence, we measured the fluorescence signals in cell nuclei with or without MC3343 or 5azadC or siRNAs against DNMT1 or DNMT3a. Given that the fluorescence signal of DXR is extinguished once the drug forms a stable bond with DNA (40), stabilized nuclear fluorescence associated with a significant decrease in the signal at 580 nm, as determined by flow cytometry (32), was observed when cells were simultaneously exposed to DXR and MC3343 compared with DXR alone but not when cells were exposed to DXR and 5azadC (Fig. 5B). Similar results were obtained when cells were simultaneously exposed to DXR and siRNA against DNMT1 or DNMT3a compared to SCR (Supplementary Fig. S1F). Accordingly, the percentage of sub-G0 cells was increased when DXR was given in association with MC3343 but not when the drug was administred with 5azadC (Fig. 5C). To further demonstrate that MC3343 but not 5azadC sustains DXR activity, we analyzed DXR-induced DNA damage represented by phosphorylated γH2AX foci (Fig. 5D). γH2AX foci were clearly evident after 1 hour of DXR treatment and were maintained up to 48 h after DXR washout when cells were exposed to MC3343 while the kinetics of γH2AX foci was not modified when cells were exposed to 5azadC, (Fig. 5D). This result indicates that inhibition of DNMTs by MC3343 limited the efficacy of the DNA damage repair process and accordingly, the

percentage of growth inhibition shifted from 32% to 65% when PDX-OS#1-C4 cells were exposed to 1 µM DXR alone or DXR and MC3343 in combination for 24 h.

## Discussion

Strategies based on the use of agents promoting cell differentiation have been successfully applied to only hematological cancers thus far (41-43). However, differentiation-based therapies would be highly desirable for solid tumors, especially for pediatric cancers or tumors resistant to traditional treatments (44). Several epigenetic regulators have emerged as valuable drivers of malignancy reversion and cell differentiation, and consequently, their pharmacological inhibitors have entered clinical evaluation (45). Among multiple mechanisms participating in the epigenetic regulation of gene expression in cancer, aberrant DNA methylation is recognized as being highly involved in the development and progression of human malignancies. Thus, DNMTs appear to be promising therapeutic targets. Here, we present the anti-proliferative and pro-differentiation effects of the novel non-nucleoside DNMTi MC3343, an analog of the quinoline-based inhibitor SGI-1027 (26), on OS. Tested in patient-derived cell lines and xenografts, the compound severely limited cell proliferation while increasing the expression of genes specifically related to osteoblastogenesis and inducing matrix mineralization. Compared to 5azadC, MC3343 had similar antiproliferative effects but was more potent in promoting differentiation. Analysis of genes involved in osteoblastogenesis after treatment indeed demonstrated the gene-specificity of MC3343, which appeared to reactivate the cascade of regulatory genes associated with osteoblastic differentiation that is aberrantly silenced in OS. This specific effect was not observed for 5azadC, which induced only general, rather unspecific re-expression of genes. The specific induction of osteoblastic differentiation is indeed very relevant for OS, which should be considered a differentiation disease (46). Transformation is thought to occur in MSCs and/or osteoprogenitors in any phase of differentiation (9, 47) and blocks the highly structured process that leads to the normal terminal differentiation of osteoblasts (46). OS molecular features suggest that both genetic and epigenetic disruptions of osteoblast differentiation pathways may occur during tumor

development. In particular, OS cells showed more hypermethylated genes than hypomethylated genes (31, 48), thus supporting the use of a DNMTi in this disease. Here, we demonstrated that differentiation was stimulated *in vitro* and *in vivo* by MC3343, which restored the balance between proliferation and differentiation, promoted OS cells toward the mature osteoblast phenotype and limited tumor growth. Although conventional OSs are high-grade, poorly differentiated lesions, well-differentiated, low-grade OSs exist and display more favorable clinical outcomes (49). As in leukemia, pro-differentiating agents may thus be exploited to transform severe cancers into more amenable afflictions (17). In addition to inhibiting the growth of OS PDXs, DNMT blockade with MC3343 also increased the chemo-sensitivity of OS cells to DXR and CDDP, two major drugs used in the treatment of OS patients that require access to DNA for activity, but not to MTX, a dihydrofolate reductase inhibitor that kills tumor cells by affecting folate homeostasis. The lack of synergism between MC3343 and MTX further supported the unique mechanism of action of MC3343. Pharmacological manipulation of DNMTs may potentiate the efficacy of cytotoxic agents that act by targeting DNA either by inducing chromatin de-condensation and increasing drug associations to DNA (38, 39) or by reverting the epigenetic silencing of genes involved in cell cycle regulation, DNA repair and apoptosis (50), which are known to largely affect tumor cell sensitivity to agents causing DNA damage. We showed that MC3343 as well as siRNA against DNMTs, was capable of increasing stable DXR bonds with DNA, and the combination of MC3343 and DXR consequently enhanced DXR-induced DNA damage and cell death and had increased efficacy against tumor growth. Generally, it is certainly true that differentiated cells are usually less sensitive to cytotoxic therapies due to their limited proliferative ability. However, MC3343, while acting as a purely cytostatic agent when used alone, increased the apoptotic activity of agents affecting DNA. Notably, none of these effects have been observed with 5azadC, further supporting the use of the novel DNMT inhibitor MC3343 in the treatment of OS.

Overall, these results demonstrate at a preclinical level that the novel DNMT inhibitor MC3343 is a very promising option for OS differentiation therapy and may be ideally considered an adjuvant agent in the treatment of patients with a poor response to pre-adjuvant chemotherapy, evaluated as a percentage of necrosis at the time of surgery (51, 52), and with unfavorable prognoses. For effective translation to preclinical studies, it will be important to fine-tune the drug dosing and timing strategies to improve outcomes and reduce toxicity. The demonstration that MC3343 treatment increases the efficacy of DXR and CDDP in killing OS cells offers the possibility of reducing the toxicity and side effects of these agents, valuable extra benefits for teenage and young adult OS patients. Nonetheless, the identification of key features able to predict which patients are likely to respond or become resistant to these drugs is highly desirable. While our preliminary data on a panel of 10 lines indicated a direct relationship between MC3343 sensitivity and DNMT1/DNMT3a expression, this relationship requires validation. In addition, considering that differentiated cells may be less sensitive to cytotoxic drugs, a careful evaluation of drug schedule and treatment timing is necessary before any possible clinical application.

## References

1. Ottaviani G, Jaffe N. The epidemiology of osteosarcoma. Cancer Treat Res. 2009;152:3-13.
2. Luetke A, Meyers PA, Lewis I, Juergens H. Osteosarcoma treatment - where do we stand? A state of the art review. Cancer Treat Rev. 2014;40:523-32.
3. Errani C, Longhi A, Rossi G, Rimondi E, Biazzo A, Toscano A, et al. Palliative therapy for osteosarcoma. Expert Rev Anticancer Ther. 2011;11:217-27.
4. Avigad S, Shukla S, Naumov I, Cohen IJ, Ash S, Meller I, et al. Aberrant methylation and reduced expression of RASSF1A in Ewing sarcoma. Pediatr Blood Cancer. 2009;53:1023-8.
5. Chou AJ, Geller DS, Gorlick R. Therapy for osteosarcoma: where do we go from here? Paediatr Drugs. 2008;10:315-27.
6. Buddingh EP, Anninga JK, Versteegh MI, Taminiau AH, Egeler RM, van Rijswijk CS, et al. Prognostic factors in pulmonary metastasized high-grade osteosarcoma. Pediatr Blood Cancer. 2010;54:216-21.
7. Martin JW, Squire JA, Zielenska M. The genetics of osteosarcoma. Sarcoma. 2012;2012:627254.
8. Geller DS, Gorlick R. Osteosarcoma: a review of diagnosis, management, and treatment strategies. Clin Adv Hematol Oncol. 2010;8:705-18.
9. Dani N, Olivero M, Mareschi K, van Duist MM, Miretti S, Cuvertino S, et al. The MET oncogene transforms human primary bone-derived cells into osteosarcomas by targeting committed osteo-progenitors. J Bone Miner Res. 2012;27:1322-34.
10. Thomas D, Kansara M. Epigenetic modifications in osteogenic differentiation and transformation. Journal of cellular biochemistry. 2006;98:757-69.
11. Siddiqi S, Mills J, Matushansky I. Epigenetic remodeling of chromatin architecture: exploring tumor differentiation therapies in mesenchymal stem cells and sarcomas. Current stem cell research & therapy. 2010;5:63-73.
12. Lopez M, Halby L, Arimondo PB. DNA Methyltransferase Inhibitors: Development and Applications. Advances in experimental medicine and biology. 2016;945:431-73.
13. Pechalrieu D, Etievant C, Arimondo PB. DNA methyltransferase inhibitors in cancer: From pharmacology to translational studies. Biochemical pharmacology. 2017;129:1-13.
14. Jurkowska RZ, Jurkowski TP, Jeltsch A. Structure and function of mammalian DNA methyltransferases. Chembiochem. 2011;12:206-22.
15. Chik F, Szyf M. Effects of specific DNMT gene depletion on cancer cell transformation and breast cancer cell invasion; toward selective DNMT inhibitors. Carcinogenesis. 2011;32:224-32.
16. Zheng YG, Wu J, Chen Z, Goodman M. Chemical regulation of epigenetic modifications: opportunities for new cancer therapy. Med Res Rev. 2008;28:645-87.
17. Fenaux P, Mufti GJ, Hellstrom-Lindberg E, Santini V, Finelli C, Giagounidis A, et al. Efficacy of azacitidine compared with that of conventional care regimens in the treatment of higher-risk myelodysplastic syndromes: a randomised, open-label, phase III study. The Lancet Oncology. 2009;10:223-32.
18. Krishnadas DK, Shapiro T, Lucas K. Complete remission following decitabine/dendritic cell vaccine for relapsed neuroblastoma. Pediatrics. 2013;131:e336-41.
19. Grishina O, Schmoor C, Dohner K, Hackanson B, Lubrich B, May AM, et al. DECIDER: prospective randomized multicenter phase II trial of low-dose decitabine (DAC) administered alone or in combination with the histone deacetylase inhibitor valproic acid (VPA) and all-trans retinoic acid (ATRA) in patients >60 years with acute myeloid leukemia who are ineligible for induction chemotherapy. BMC cancer. 2015;15:430.
20. Locklin RM, Oreffo RO, Triffitt JT. Modulation of osteogenic differentiation in human skeletal cells in Vitro by 5-azacytidine. Cell Biol Int. 1998;22:207-15.

21. Al-Romaih K, Sadikovic B, Yoshimoto M, Wang Y, Zielenska M, Squire JA. Decitabine-induced demethylation of 5' CpG island in GADD45A leads to apoptosis in osteosarcoma cells. Neoplasia. 2008;10:471-80.
22. Al-Romaih K, Somers GR, Bayani J, Hughes S, Prasad M, Cutz JC, et al. Modulation by decitabine of gene expression and growth of osteosarcoma U2OS cells in vitro and in xenografts: identification of apoptotic genes as targets for demethylation. Cancer Cell Int. 2007;7:14.
23. Thayanithy V, Park C, Sarver AL, Kartha RV, Korpela DM, Graef AJ, et al. Combinatorial treatment of DNA and chromatin-modifying drugs cause cell death in human and canine osteosarcoma cell lines. PLoS One. 2012;7:e43720.
24. Nestheide S, Bridge JA, Barnes M, Frayer R, Sumegi J. Pharmacologic inhibition of epigenetic modification reveals targets of aberrant promoter methylation in Ewing sarcoma. Pediatr Blood Cancer. 2013;60:1437-46.
25. Li Y, Huang Y, Lv Y, Meng G, Guo QN. Epigenetic regulation of the pro-apoptosis gene TSSC3 in human osteosarcoma cells. Biomed Pharmacother. 2014;68:45-50.
26. Datta J, Ghoshal K, Denny WA, Gamage SA, Brooke DG, Phiasivongsa P, et al. A new class of quinoline-based DNA hypomethylating agents reactivates tumor suppressor genes by blocking DNA methyltransferase 1 activity and inducing its degradation. Cancer Res. 2009;69:4277-85.
27. Valente S, Liu Y, Schnekenburger M, Zwergel C, Cosconati S, Gros C, et al. Selective non-nucleoside inhibitors of human DNA methyltransferases active in cancer including in cancer stem cells. J Med Chem. 2014;57:701-13.
28. Gros C, Fleury L, Nahoum V, Faux C, Valente S, Labella D, et al. New insights on the mechanism of quinoline-based DNA Methyltransferase inhibitors. J Biol Chem. 2015;290:6293-302.
29. Benini S, Baldini N, Manara MC, Chano T, Serra M, Rizzi S, et al. Redundancy of autocrine loops in human osteosarcoma cells. Int J Cancer. 1999;80:581-8.
30. Ottaviano L, Schaefer KL, Gajewski M, Huckenbeck W, Baldus S, Rogel U, et al. Molecular characterization of commonly used cell lines for bone tumor research: a trans-European EuroBoNet effort. Genes Chromosomes Cancer. 2010;49:40-51.
31. Kresse SH, Rydbeck H, Skarn M, Namlos HM, Barragan-Polania AH, Cleton-Jansen AM, et al. Integrative analysis reveals relationships of genetic and epigenetic alterations in osteosarcoma. PLoS One. 2012;7:e48262.
32. Baldini N, Scotlandi K, Serra M, Kusuzaki K, Shikita T, Manara MC, et al. Adriamycin binding assay: a valuable chemosensitivity test in human osteosarcoma. Journal of cancer research and clinical oncology. 1992;119:121-6.
33. Manara MC, Nicoletti G, Zambelli D, Ventura S, Guerzoni C, Landuzzi L, et al. NVP-BEZ235 as a new therapeutic option for sarcomas. Clin Cancer Res. 2010;16:530-40.
34. Nomura T, Tamaoki N, Takakura A, Suemizu H. Basic concept of development and practical application of animal models for human diseases. Current topics in microbiology and immunology. 2008;324:1-24.
35. Chou TC, Motzer RJ, Tong Y, Bosl GJ. Computerized quantitation of synergism and antagonism of taxol, topotecan, and cisplatin against human teratocarcinoma cell growth: a rational approach to clinical protocol design. Journal of the National Cancer Institute. 1994;86:1517-24.
36. Sciandra M, Marino MT, Manara MC, Guerzoni C, Grano M, Oranger A, et al. CD99 drives terminal differentiation of osteosarcoma cells by acting as a spatial regulator of ERK 1/2. J Bone Miner Res. 2014;29:1295-309.
37. Das Thakur M, Pryer NK, Singh M. Mouse tumour models to guide drug development and identify resistance mechanisms. J Pathol. 2014;232:103-11.
38. Marchion DC, Bicaku E, Daud AI, Sullivan DM, Munster PN. Valproic acid alters chromatin structure by regulation of chromatin modulation proteins. Cancer Res. 2005;65:3815-22.
39. Li J, Hao D, Wang L, Wang H, Wang Y, Zhao Z, et al. Epigenetic targeting drugs potentiate chemotherapeutic effects in solid tumor therapy. Sci Rep. 2017;7:4035.

40. Chen NT, Wu CY, Chung CY, Hwu Y, Cheng SH, Mou CY, et al. Probing the dynamics of doxorubicin-DNA intercalation during the initial activation of apoptosis by fluorescence lifetime imaging microscopy (FLIM). PLoS One. 2012;7:e44947.
41. Petrie K, Zelent A, Waxman S. Differentiation therapy of acute myeloid leukemia: past, present and future. Current opinion in hematology. 2009;16:84-91.
42. Kulling PM, Olson KC, Olson TL, Feith DJ, Loughran TP, Jr. Vitamin D in hematological disorders and malignancies. European journal of haematology. 2017;98:187-97.
43. Chistiakov DA, Myasoedova VA, Orekhov AN, Bobryshev YV. Epigenetically active drugs inhibiting DNA methylation and histone deacetylation. Current pharmaceutical design. 2016.
44. Cruz FD, Matushansky I. Solid tumor differentiation therapy - is it possible? Oncotarget. 2012;3:559-67.
45. Biswas S, Rao CM. Epigenetics in cancer: Fundamentals and Beyond. Pharmacology & therapeutics. 2017;173:118-34.
46. Tang N, Song WX, Luo J, Haydon RC, He TC. Osteosarcoma development and stem cell differentiation. Clin Orthop Relat Res. 2008;466:2114-30.
47. Matushansky I, Hernando E, Socci ND, Mills JE, Matos TA, Edgar MA, et al. Derivation of sarcomas from mesenchymal stem cells via inactivation of the Wnt pathway. J Clin Invest. 2007;117:3248-57.
48. Zhang W, Han S, Sun K. Combined analysis of gene expression, miRNA expression and DNA methylation profiles of osteosarcoma. Oncol Rep. 2017;37:1175-81.
49. Thomas DM, Johnson SA, Sims NA, Trivett MK, Slavin JL, Rubin BP, et al. Terminal osteoblast differentiation, mediated by runx2 and p27KIP1, is disrupted in osteosarcoma. The Journal of cell biology. 2004;167:925-34.
50. Muvarak NE, Chowdhury K, Xia L, Robert C, Choi EY, Cai Y, et al. Enhancing the Cytotoxic Effects of PARP Inhibitors with DNA Demethylating Agents - A Potential Therapy for Cancer. Cancer Cell. 2016;30:637-50.
51. Ferrari S, Serra M. An update on chemotherapy for osteosarcoma. Expert Opin Pharmacother. 2015;16:2727-36.
52. Isakoff MS, Bielack SS, Meltzer P, Gorlick R. Osteosarcoma: Current Treatment and a Collaborative Pathway to Success. J Clin Oncol. 2015;33:3029-35.

**Table 1. *In vitro* efficacy of MC3343 and 5azadC in relation to the basal level of DNMTs expression in OS cell lines.**

| Cell line | $IC_{50}$*, µM | | DNMT1** | DNMT3a** | DNMT3b** |
|---|---|---|---|---|---|
| | MC3343 | 5azadC | | | |
| **Saos-2** | 5.6±1.6 | 0.7±0.1 | 0.50±0.04 | 1.02±0.04 | 0.39±0.08 |
| **IOR/OS14** | 5.3±0.2 | >30 | 0.47±0.05 | 0.81±0.01 | 0.60±0.11 |
| **MG-63** | 6.1±0.7 | 0.23±0.2 | 1.05±0.13 | 0.72±0.21 | 0.39±0.14 |
| **IOR/OS9** | 8.6±1.5 | 6.6±3.9 | 0.38±0.14 | 0.33±0.19 | 0.23±0.10 |
| **IOR/OS10** | 7.7±3.1 | 0.9±0.6 | 0.25±0.08 | 0.31±0.12 | 0.35±0.23 |
| **U-2 OS** | 11.8±2.5 | 0.7±0.2 | 0.17±0.17 | 0.13±0.16 | 0.72±0.10 |
| **IOR/OS20** | 14.5±2.1 | 13.3±3.5 | 0.20±0.08 | 0.20±0.09 | 0.51±0.15 |
| **IOR/SARG** | 5.1±0.2 | 5.5±0.8 | 0.59±0.03 | 2.07±0.04 | 1.28±0.52 |
| **PDX-OS#1-C4*** ** | 6.3 ± 0.4 | 0.5 ±0.3 | 0.54±0.17 | 0.32±0.10 | 0.17±0.19 |
| **PDX-OS#2-C2*** ** | 6.1±1.6 | 15.4±1.6 | 0.47±0.10 | 1.47±0.12 | 0.65±0.12 |

* Cells were exposed to increasing concentrations of MC3343 or 5azadC for 96 h. Data represent the mean ± SE of three independent experiments. $IC_{50}$= drug concentration inducing 50% of growth inhibition with respect to the control (untreated cells).

** DNMTs expression values are indicated as densitometry records (normalized to actin signals: $OD*mm^2/OD*mm^2$ actin) ± SE

*** PDX-OS#1-C4 and PDX-OS#2-C2 indicated cell lines obtained from the fourth or second passage in the mice of PDX-OS#1 and PDX-OS#2, respectively.

## Figure legends

**Figure 1. MC3343 efficiently inhibits the activity and expression of DNMTs in OS cells. A, B,** Western blot analysis (**A**) and immunofluorescence staining (**B**) of DNMT1, DNMT3a and DNMT3b in untreated (CTRL), MC3343-treated (3-10 µM) and 5azadC-treated (1-10 µM) Saos-2 cells. Equal loading was monitored by anti-actin blotting. Digital images were acquired under identical conditions at the same time using image analysis software (NIS Elements, Nikon). Scale bars: 20 µm. **C**, Effects on DNMT activity measured by the EpiQuik DNA Methyltransferase Activity assay (*p<0.05; **p<0.01, Student's t test).

**Figure 2. MC3343 inhibits OS cell proliferation. A**, Percentage of Ki-67-positive cells among untreated (white bars), MC3343 (3-10 µM; light and dark grey respectively) or 5azadC treated (1-10 µM for Saos-2 and IOR/OS9 cells or 0.1-1 µM for MG-63 cells; light and dark grey respectively) OS cells ( *p<0,05, **p<0.01, *** p< 0.001, Student's t test). **B**, Western blot analysis of DNMT1, cyclin D1, pRb (S795, S807/811) and total Rb after 48 h of exposure to MC3343 or 5azadC. Equal loading was monitored by anti-actin blotting. Blots are representative of at least two independent experiments**. C,** Cell cycle analysis of three representative OS cell lines after 48 h of exposure to MC3343 as determined by flow cytometry.

**Figure 3. MC3343 drives OS cells toward an osteoblast-differentiated phenotype. A,** Evaluation of Saos-2 cell growth after exposure to MC3343 or 5azadC in differentiating medium by vital counting with Trypan blue. Data are presented as the mean ± SE of three separate experiments (*** p< 0.001, Student's t test). **B**, Mineralized matrix formation by Saos-2 cells after exposure to MC3343 or 5azadC in differentiation medium as measured by ARS quantification. Data are normalized to cell number and are presented as the mean ± SE of three separate experiments (***

p< 0.001, Student's t test). **C**, RT-qPCR expression of representative osteoblast differentiation markers in Saos-2 or PDX-OS#1-C4 cells after treatment with MC3343 or 5azadC in differentiating conditions. PDX-OS#1-C4 cell line is derived from the fourth *in vivo* passage of PDX-OS#1. COL1A2, ALPL, and OCN are displayed to indicate the early, intermediate and late stages of the osteoblastic differentiation process, respectively. Expression levels of target genes (RQ) were normalized to GAPDH expression level and the results are expressed as: $2^{-\Delta\Delta Ct}$, where ΔCt = Ct target gene – Ct GAPDH and ΔΔCt = ΔCt sample - ΔCt calibrator (untreated cells at each time point). All samples were run in triplicate for each experiment. Data are presented as the mean ± SE of three separate experiments (* p<0.05, ** p<0.01, *** p< 0.001, Student's t test) **D**, Evaluation of ALPL activity by histochemical analysis after 14 days of exposure to MC3343 or 5azadC in differentiating conditions. Representative images are shown (NIS Elements, Nikon). Scale bars: 200 µm.

**Figure 4. MC3343 inhibits tumor growth and induces osteoblastic differentiation in OS PDXs. A**, Inhibition of PDX-OS#1 tumor growth *in vivo*. Drugs were administered as follows: 20 mg/kg MC3343 (n = 7) or 0.8 mg/kg 5azadC (n = 4) daily 5 times/week for 14 days. Student's t test: * p< 0.05; ** p< 0.01; compared with the controls (vehicle n = 8). Data are presented as the mean tumor volume ± SE. **B**, Percentage of Ki-67-positive cells in untreated and treated tumors (** p<0.01, *** p< 0.001, Student's t test). **C**, Representative immunohistochemical images of DNMT1, Ki-67, OCN and von Kossa staining in untreated and treated tumors are shown. Scale bars: 50 µm.

**Figure 5. MC3343 potentiates OS cell sensitivity to cytotoxic agents acting by targeting DNA. A,** *In vivo* inhibition of PDX-OS#1 tumor growth by the MC3343 and DXR combination. Drugs were administered as follows: DXR (50 µg/injection for 2 days, n = 5), MC3343 (20 mg/kg for 14d, n = 5), DXR + MC3343 (n = 8). Student's t test: * p < 0.05; ** p < 0.01; *** p <0.001 compared to

untreated mice (n = 9). **B,** Mean fluorescence intensity (MFI) of DXR within nuclei of PDX-OS#1-C4 cells treated with DXR (10 µM) alone or in combination with MC3343 (10 µM) or 5azadC (1 µM) quantified by NIS-Elements AR 3.10 (Nikon) software. Plots are presented as the mean ± SE after 1 h of drug exposure; ***p<0.001, Student's t test. Representative images are shown. Scale bars: 20 µm. **C**, Percentage of subG0 PDX-OS#1-C4 cells upon treatment with DXR (1 µM) for 3 h and subsequent washout with IMDM (CTRL), MC3343 (10 µM) or 5azadC (1 µM) for 24 h. **D,** γ-H2AX immunofluorescence staining in PDX-OS#1-C4 cells after 1 h of exposure to 1 µM DXR and washout with complete medium with or without MC3343 (10 µM) or 5azadC (1 µM) for 6-48 h. The percentage of positive cells was obtained by flow cytometry analysis (*p<0.05, Student's t test). Representative images are shown. Scale bars: 20 µm.

Author Manuscript Published OnlineFirst on June 29, 2018; DOI: 10.1158/1535-7163.MCT-17-0818
Author manuscripts have been peer reviewed and accepted for publication but have not yet been edited.

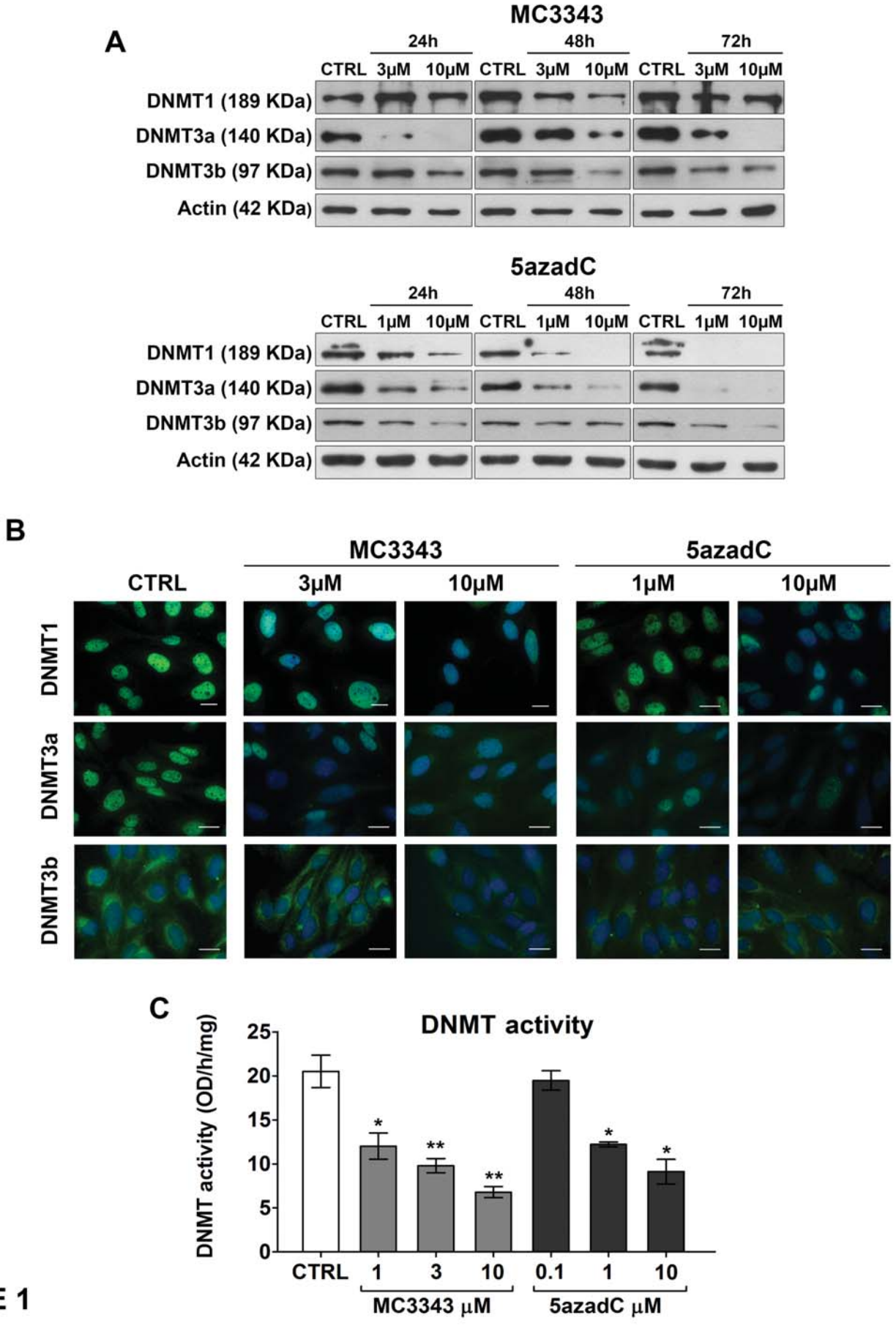


FIGURE 1

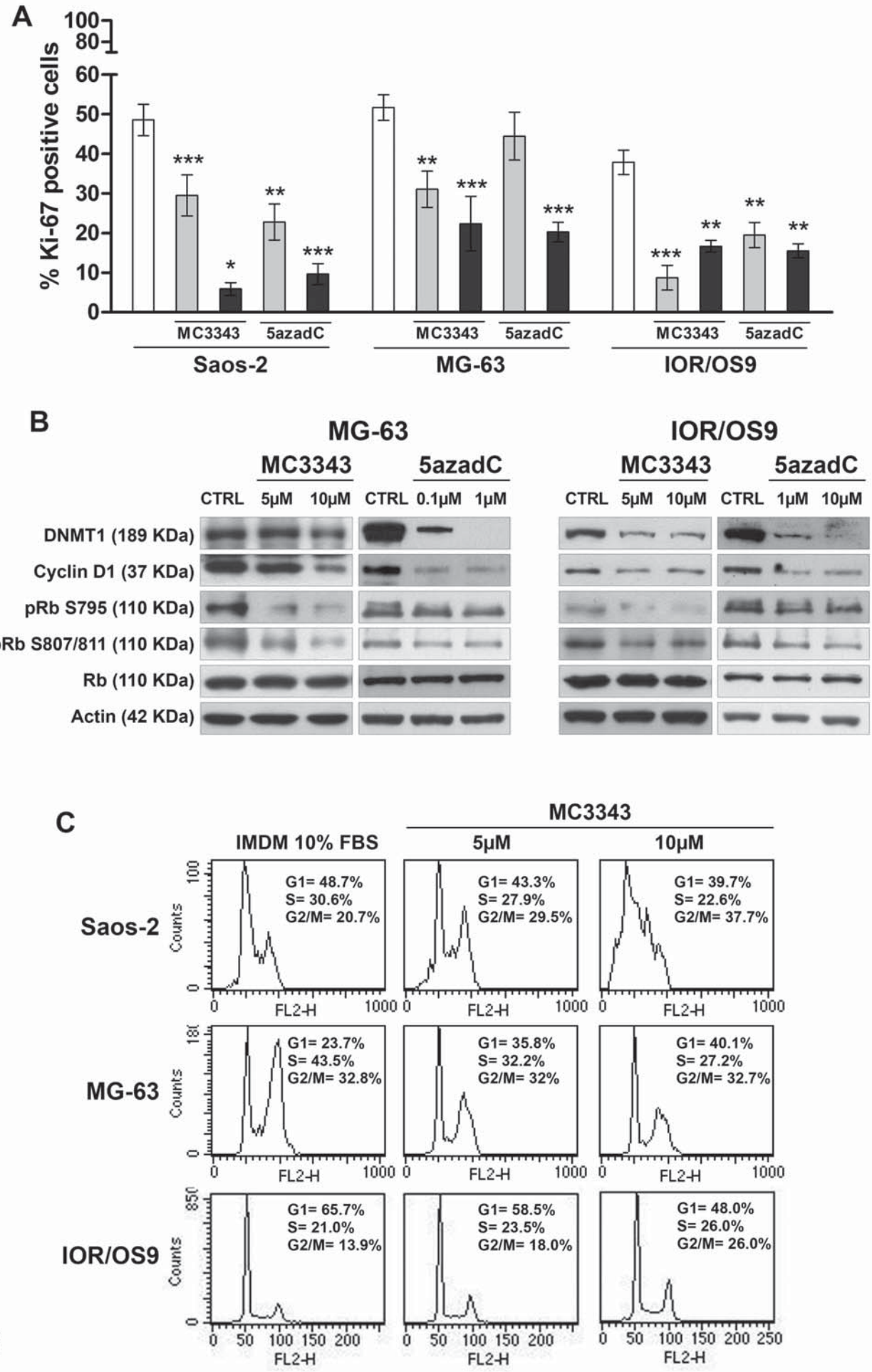


FIGURE 2

Author Manuscript Published OnlineFirst on June 29, 2018; DOI: 10.1158/1535-7163.MCT-17-0818
Author manuscripts have been peer reviewed and accepted for publication but have not yet been edited.

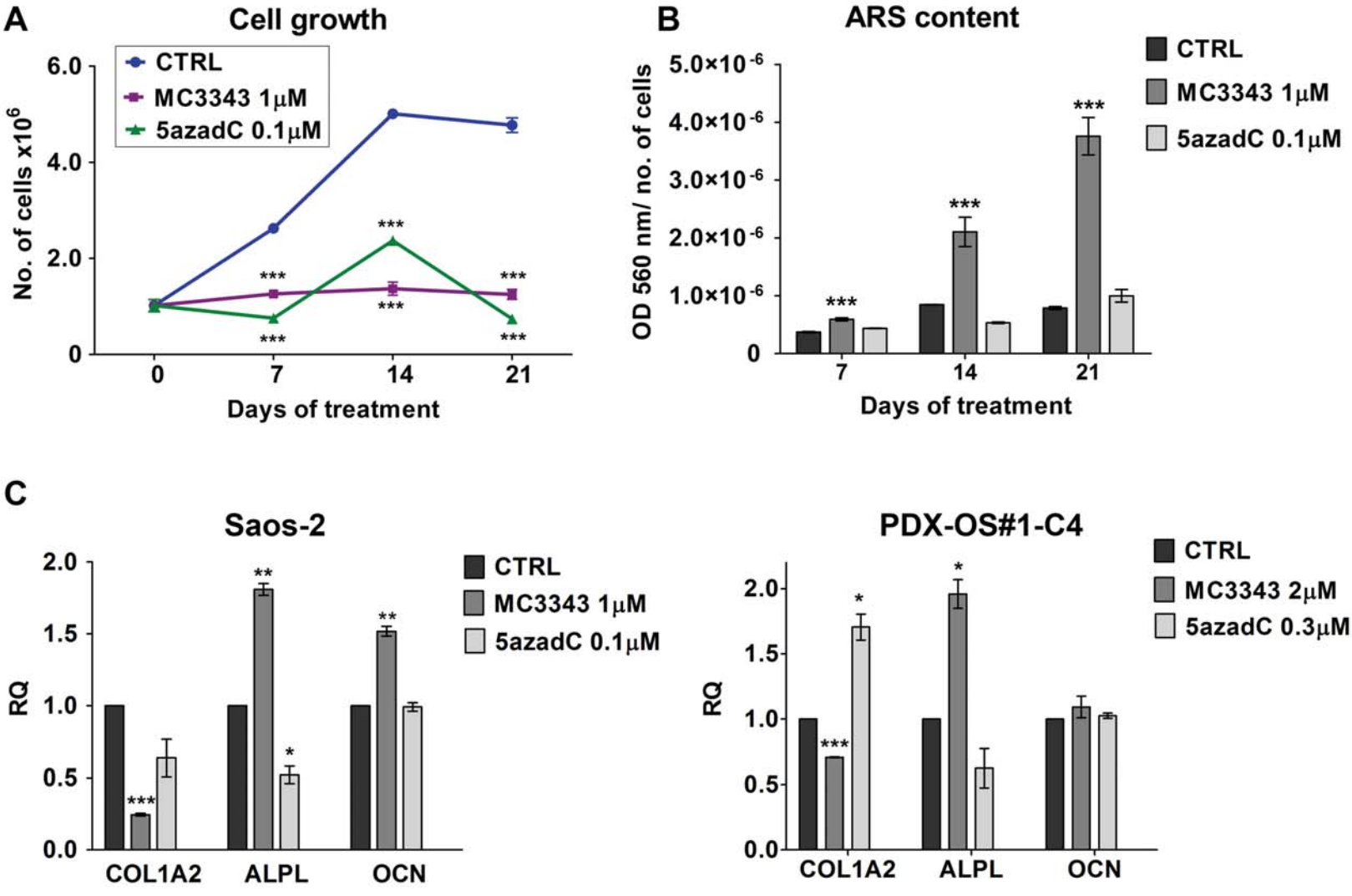


FIGURE 3

Author Manuscript Published OnlineFirst on June 29, 2018; DOI: 10.1158/1535-7163.MCT-17-0818
Author manuscripts have been peer reviewed and accepted for publication but have not yet been edited.

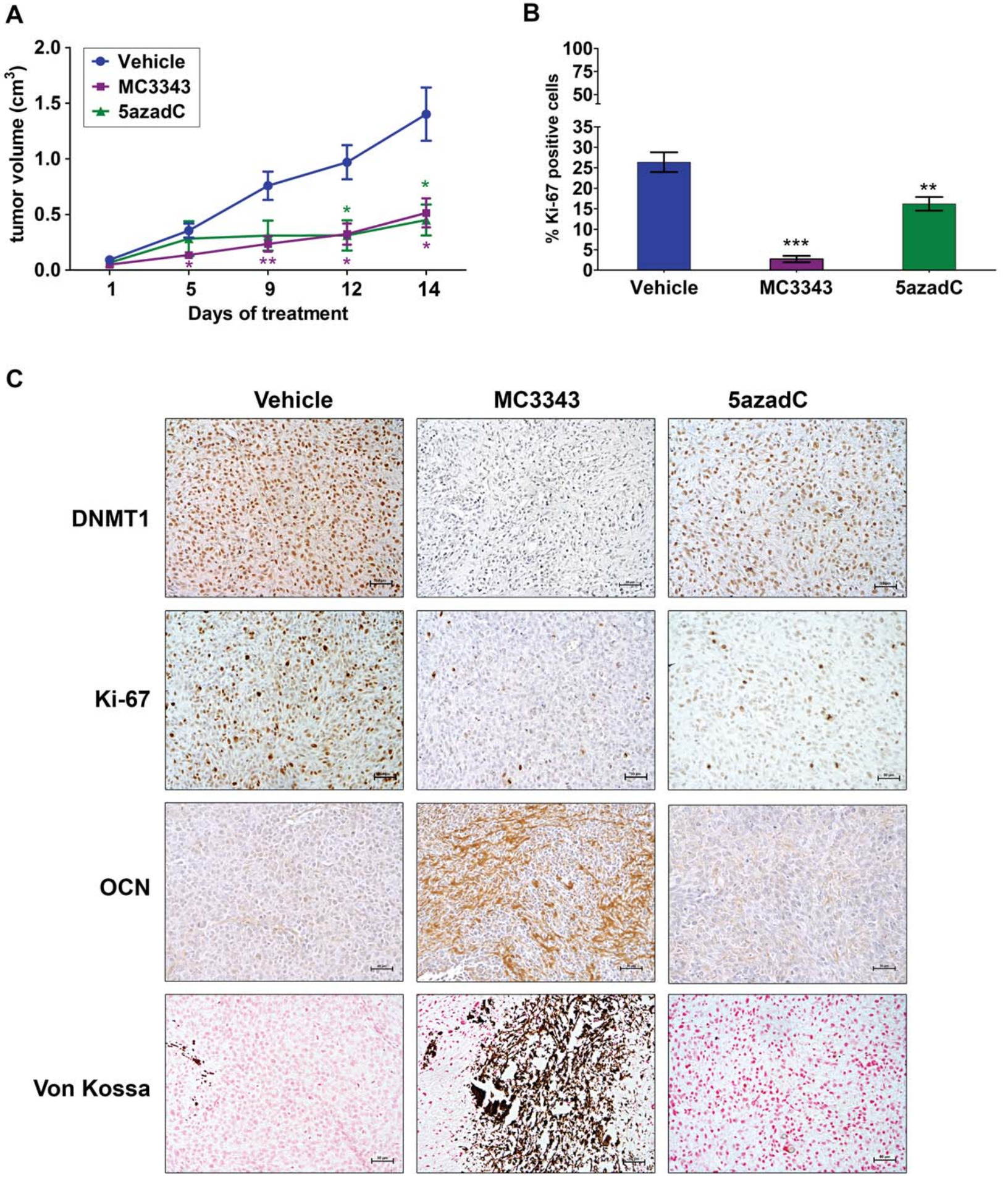


FIGURE 4

Author Manuscript Published OnlineFirst on June 29, 2018; DOI: 10.1158/1535-7163.MCT-17-0818
Author manuscripts have been peer reviewed and accepted for publication but have not yet been edited.

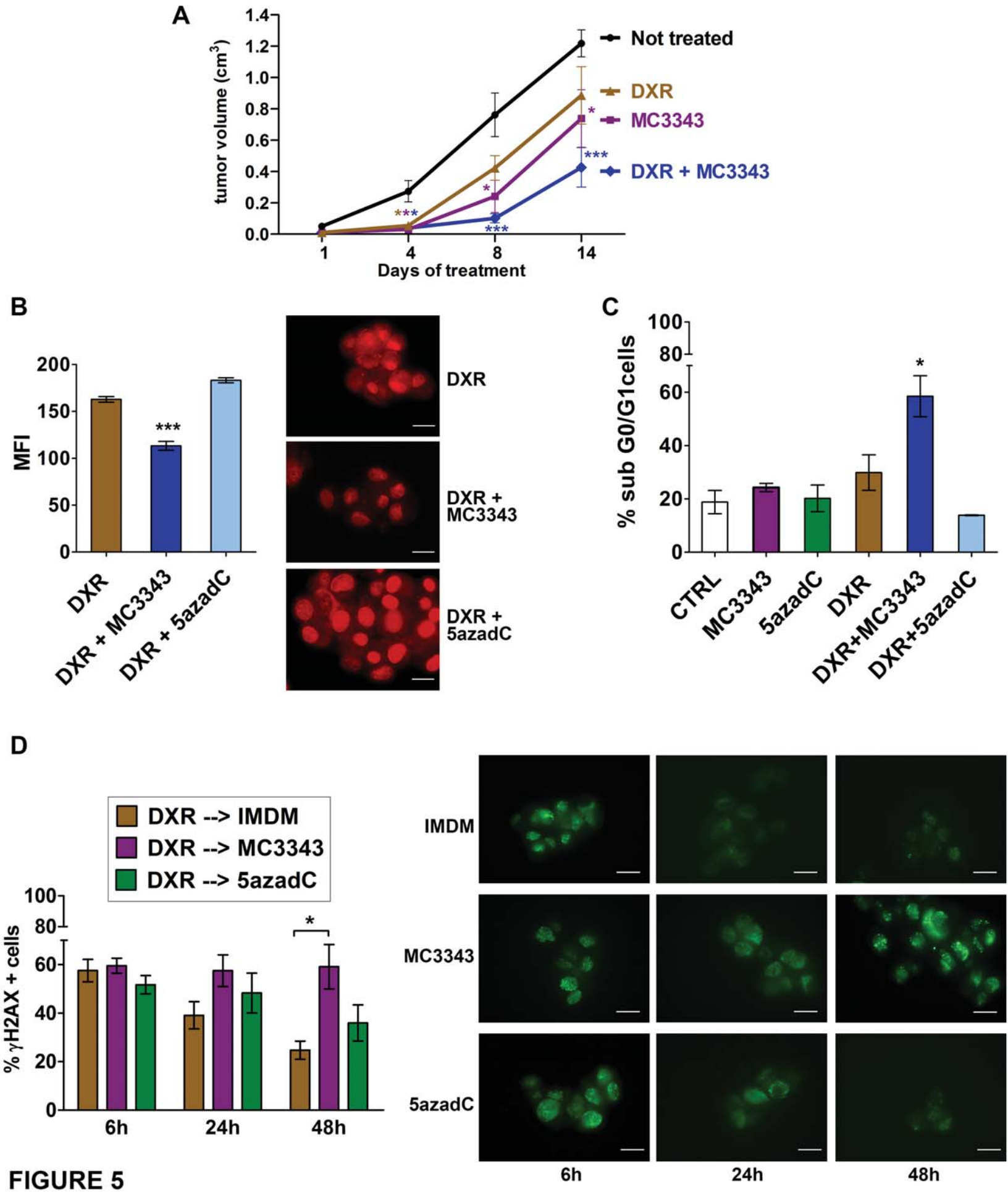


FIGURE 5

AACR American Association for Cancer Research

Molecular Cancer Therapeutics

# A Quinoline-Based DNA Methyltransferase Inhibitor as a Possible Adjuvant in Osteosarcoma Therapy

Maria Cristina Manara, Sergio Valente, Camilla Cristalli, et al.

*Mol Cancer Ther* Published OnlineFirst June 29, 2018.